Functional and structural roles of the glutathione-binding residues in maize (*Zea mays*) glutathione S-transferase I

Nikolaos E. LABROU*, Luciane V. MELLO† and Yannis D. CLONIS*[1]

*Laboratory of Enzyme Technology, Department of Agricultural Biotechnology, Agricultural University of Athens, 75 Iera Odos Street, GR-11855 Athens, Greece, and †Embrapa-Genetics Resources and Biotechnology, Estação Parque Biológico, Final W5, Asa Norte, 70770-900, Brasília, DF, Brazil

The isoenzyme glutathione S-transferase (GST) I from maize (*Zea mays*) was cloned and expressed in *Escherichia coli*, and its catalytic mechanism was investigated by site-directed mutagenesis and dynamic studies. The results showed that the enzyme promotes proton dissociation from the GSH thiol and creates a thiolate anion with high nucleophilic reactivity by lowering the pK_a of the thiol from 8.7 to 6.2. Steady-state kinetics fit well to a rapid equilibrium, random sequential Bi Bi mechanism, with intrasubunit modulation between the GSH binding site (G-site) and the electrophile binding site (H-site). The rate-limiting step of the reaction is viscosity-dependent, and thermodynamic data suggest that product release is rate-limiting. Five residues of GST I (Ser^{11}, His^{40}, Lys^{41}, Gln^{53} and Ser^{67}), which are located in the G-site, were individually replaced with alanine and their structural and functional roles in the 1-chloro-2,4-dinitrobenzene (CDNB) conjugation reaction were investigated. On the basis of steady-state kinetics, difference spectroscopy and limited proteolysis studies it is concluded that these residues: (1) contribute to the affinity of the G-site for GSH, as they are involved in side-chain interaction with GSH; (2) influence GSH thiol ionization, and thus its reactivity; (3) participate in k_{cat} regulation by affecting the rate-limiting step of the reaction; and (4) in the cases of His^{40}, Lys^{41} and Gln^{53} play an important role in the structural integrity of, and probably in the flexibility of, the highly mobile short 3_{10}-helical segment of α-helix 2 (residues 35–46), as shown by limited proteolysis experiments. These structural perturbations are probably transmitted to the H-site through changes in Phe^{35} conformation. This accounts for the modulation of K_m^{CDNB} by His^{40}, Lys^{41} and Gln^{53}, and also for the intrasubunit communication between the G- and H-sites. Computer simulations using CONCOORD were applied to maize GST I monomer and dimer structures, each with bound lactoylglutathione, and the results were analysed by the essential dynamics technique. Differences in dynamics were found between the monomer and the dimer simulations showing the importance of using the whole structure in dynamic analysis. The results obtained confirm that the short 3_{10}-helical segment of α-helix 2 (residues 35–46) undergoes the most significant structural rearrangements. These rearrangements are discussed in terms of enzyme catalytic mechanism.

Key words: essential dynamics, herbicide detoxification, molecular dynamics, protein engineering.

INTRODUCTION

The glutathione S-transferases (GSTs; EC 2.5.1.18) are a widely distributed family of detoxifying dimeric enzymes found in all vertebrates, plants, insects, nematodes, yeast and aerobic bacteria [1,2]. GST catalyses the nucleophilic attack of the sulphur atom of the tripeptide GSH on electrophilic groups of a variety of hydrophobic substrates, including herbicides, insecticides and carcinogens, resulting either in addition or substitution reactions depending on the nature of the substrate [1,2,3]. The conjugation of GSH to such molecules increases their solubility and facilitates further metabolic processing [4].

The catalysis of nucleophilic aromatic substitution reactions can be divided into steps involving substrate binding to the enzyme active site, activation of GSH by deprotonation of the thiol to form the nucleophilic thiolate anion and nucleophilic attack by the thiolate at the substrate electrophilic centre [5–7]. The enzymic mechanism involves tyrosine- (κ, σ, α, μ and π classes) or serine- (θ and δ classes) mediated deprotonation of the thiol group of the bound GSH [2,3,5–7]. Very significant advances in our understanding of the structure and mechanism of GSTs have been elucidated, but important questions with regard to the determinants of the reaction pathway that influence k_{cat} and K_m still need to be addressed [2,3].

The interest in plant GSTs derives from their agronomic value [8]. It has been demonstrated that GSH conjugation for a variety of herbicides is the major resistance and selectivity factor in plants, and provides a tool to control weeds in agronomic crops [1,8,9]. The first GST reported to participate in herbicide metabolism is that of maize (*Zea mays*), where six isoforms termed GST I–GST VI have been characterized in some detail [1,9]. Of all the GSTs, the isoenzyme GST I shows the most significant activity towards the two most important classes of herbicide, triazines and chloroacetamides, as studied with the compounds atrazine, alachlor and metalachlor [9]. Due to the ability of GST I to detoxify herbicides, and considering a market for maize herbicides of approx. $1.5 billion per year [10], the study of the structure and function of maize GSTs is of practical importance. So far, three crystal structures of plant GSTs have been elucidated. These are the *Arabidopsis thaliana* GST [10], maize GST I [11] and maize GST III [12]. In all three enzymes the overall topology is very similar, but each structure exhibits unique

Abbreviations used: CDNB, 1-chloro-2,4-dinitrobenzene; G-site, GSH binding site; GST, glutathione S-transferase; H-site, electrophile binding site; Ni-NTA, Ni^{2+}-nitrilotriacetate.

[1] To whom correspondence should be addressed (e-mail clonis@aua.gr).

features, particularly concerning the substrate recognition site [11,13]. For maize GST I two features have been reported, based on the crystal structure [13], to contribute to catalytic efficiency towards electrophile substrates: (1) the size and shape of the electrophile binding site (H-site), which is determined by the hydrophobic residues Met^{10}, Trp^{12}, Phe^{35} and Ile^{118}; and (2) the flexibility in the upper part of the H-site that is modulated by Gly^{123} and Gly^{124} [11,13].

Despite the agronomic potential of plant GSTs, this family of GSTs is poorly characterized, compared with other GST families. Kinetic or mutagenesis studies concerning the catalytic mechanism of plant GSTs have not been reported so far. Thus detailed study of the catalytic mechanism operating by this family of enzymes is of academic interest and practical importance. In addition, θ class GSTs are believed to be the most similar to the ancestral GST from which the α, μ and π classes have evolved [14]. Thus investigation of θ class GSTs would be very important from an evolutionary point of view. In the present study we address questions regarding the functional and structural role of GSH binding residues of GST I, that have not attracted significant attention over recent years [15]. Their role, as will be shown in the present work, is not just limited to the binding process, since they also contribute significantly to the catalysis. The results of the present work will form the basis for a rational design of new engineered GSTs with altered specificity and enhanced catalytic efficiency towards herbicides, and will help in the design of new more selective herbicides.

MATERIALS AND METHODS

Materials

A polyadenylated mRNA purification kit was obtained from Ingenius (R&D Systems Europe Ltd, Abingdon, Oxfordshire, U.K.). First-strand cDNA synthesis kits, dNTPs and restriction enzymes were obtained from Boehringer Mannheim (Mannheim, Germany). Unique-site elimination mutagenesis kits, and the expression vector pKK223-3 were purchased from Pharmacia (Uppsala, Sweden). GSH and 1-chloro-2,4-dinitrobenzene (CDNB) were obtained from Sigma (Steinheim, Germany). XL1-Blue *Escherichia coli* cells and *Pfu* DNA polymerase were purchased from Stratagene (La Jolla, CA, U.S.A.). Ni^{2+}-nitrilotriacetate (Ni-NTA) adsorbent was obtained from Qiagen (Crawley, West Sussex, U.K.).

Methods

Plant material and growth conditions

Sterilized maize seeds (Kelvedon Glory) were germinated for 6 days at 25 °C on vermiculite with a 16 h photoperiod.

Molecular cloning

Polyadenylated mRNA was purified from crude plant roots using an RNA isolation kit according to the manufacturer's instructions (Ingenius, R&D Systems Europe Ltd). First-strand cDNA synthesis was performed using an oligo-p$(dT)_{15}$ primer and avian myeloblastosis virus reverse transcriptase according to the manufacturer's recommendations (Boehringer Mannheim). The PCR primers 5′-TTTTGAATTCGATGGCTCCGATGA-AGCTGTACGGGGCG-3′ (forward primer) and 5′-AGCAG-ATGGCTTCATCAGGGCAGC-3′ (reverse primer) were designed according to the GST I gene sequence described by Grove et al. [16]. An *Eco*RI restriction site was introduced at the 5′ end of the forward primer. The PCR was carried out in a total volume of 50 μl containing 4 pmol of each primer, 1 μg of template cDNA, 0.2 mM each dNTP, 5 μl of 10× *Pfu* buffer and 0.6 units of *Pfu* DNA polymerase (Stratagene). The PCR procedure comprised 30 cycles of 45 s at 95 °C, 1 min at 68 °C and 2 min at 72 °C. A final extension time at 72 °C for 10 min was performed after the 30 cycles. The PCR products were run on a 1.2% (w/v) agarose gel and a fragment of 653 bp was excised, purified by adsorption to silica beads and ligated to the oligonucleotide cassette encoding a 6× histidine tag, in which a Factor Xa proteolytic site and an *Eco*RI restriction site were introduced at the 5′ and 3′ ends respectively: 5′-ATCGAAG-GTCGTCATCACCATCACCATCACTAGG-3′ and 3′-TAG-CTTCCAGCAGTAGTGGTAGTAGTAGTGATCCTTAA-5′.

The ligation product was gel-purified, restricted with *Eco*RI and cloned into a pKK223-3 expression vector, which was previously restricted with *Eco*RI. The resulting expression construct, pGST I, was used to transform competent *E. coli* XL1-Blue cells. Nucleotide sequencing was performed along both strands using an Applied Biosystems Sequencer 373A.

Site-directed mutagenesis

Site-directed mutagenesis was performed according to the unique-site elimination method described by Deng and Nickoloff [17]. The oligonucleotide primer sequences used were as follows: for the $Ser^{11} \rightarrow$ Ala mutation, 5′-GCG GTG ATG GCG TGG AAC GTG-3′; for the $His^{40} \rightarrow$ Ala mutation, 5′-ACC GCC GAG GCC AAG AGC CCC G-3′; for the $Lys^{41} \rightarrow$ Ala mutation, 5′-GCC GAG CAC GCG AGC CCC GAG-3′; for the $Gln^{53} \rightarrow$ Ala mutation, 5′-CCG TTT GGT GCG GTT CCA GCT CTG-3′; and for the $Ser^{67} \rightarrow$ Ala mutation, 5′-CTC TTC GAA GCA CGC GCA ATC TGC-3′. The selection primer sequence was as follows: 5′-GAA TTC TCG TGG ATC CGT CGA CCT-3′. This primer contains a mutation in a unique *Sma*I restriction site of the pGST I vector. The primers were phosphorylated before use with polynucleotide kinase and were then used in pairs with one mutant primer and the selection primer in each mutagenesis reaction. The expression construct pGST I encoding maize GST I was used as template DNA in all mutagenesis reactions. All mutations were verified by DNA sequencing on an Applied Biosystems Sequencer 373A with the DyeDeoxy Terminator Cycle sequencing kit.

Heterologous expression and purification of maize GST I

E. coli cells, harbouring plasmid pGST I, were grown at 37 °C in 1 litre of Luria–Bertani medium containing 100 μg/ml ampicillin [18,19]. The synthesis of GST was induced by the addition of 1 mM isopropyl β-D-thiogalactoside when the attenuance (D) at 600 nm was 0.6. Following induction for 3 h cells were harvested (approx. 3 g) by centrifugation at 10000 ***g*** for 10 min, resuspended in 9 ml of 50 mM potassium phosphate buffer (pH 8.0) containing 0.3 M NaCl, sonicated and centrifuged at 10000 ***g*** for 20 min. The supernatant was collected and was loaded on to a column of Ni-NTA adsorbent (1 ml), which was previously equilibrated with 50 mM potassium phosphate buffer (pH 8.0) containing 0.3 M NaCl. Non-adsorbed protein was washed off with 10 ml of equilibration buffer, followed by 20 ml of 50 mM potassium phosphate buffer (pH 6.2) containing 0.3 M NaCl and 10% (v/v) glycerol. Bound GST I was eluted with equilibration buffer containing 0.1 M imidazole (5 ml). Collected fractions (1 ml) were assayed for GST I activity and protein (A_{280}), and were dialysed overnight against 50 mM potassium phosphate buffer (pH 8.0) containing 0.3 M NaCl.

The Ni-NTA chromatography step was then repeated as described above. Protein purity was judged by SDS/PAGE.

Computer simulations

The trajectories were produced using the CONCOORD method [20,21], applied to maize GST I with bound lactoylglutathione (pdb code 1axd) [11] and human GST P1-1 complexed with *S*-hexylglutathione (pdb code 1gss) [22]. The CONCOORD program generates random protein structures fulfilling a set of upper and lower interatomic distance limits. These limits are derived from experimental structures through measurement of distances and prediction of interaction strength. Thus the separation of strongly interacting atoms is allowed to vary only slightly from the observed value, whereas weaker interactions are accorded more relaxed limits. Special consideration is given to interacting atoms within the same secondary structure element, in order to ensure the preservation of secondary structure. While detailed aspects of dynamic variation may not be reproduced by this method, good qualitative agreement has been found between results of conventional molecular dynamics and CONCOORD simulations [20]. CONCOORD is particularly applicable to large systems, where conventional molecular dynamics would require unfeasibly large amounts of computer time, and is finding an increasing number of applications [21].

Structures (500) were generated for each of the GSTs analysed. These were treated as a molecular dynamics trajectory [20], and were analysed using the essential dynamics method [23]. The essential dynamics method is based on the diagonalization of the covariance matrix [23,24]. The central hypothesis of this method is that only the motions along the eigenvectors with large eigenvalues are important for describing the functionally significant motions in the protein.

Electrophoresis

Protein purity was judged by SDS/PAGE using 12.5% (w/v) polyacrylamide for the running gel and 2.5% (w/v) polyacrylamide for the stacking gel, according to the method of Laemmli [25]. The protein bands were stained with Coomassie Brilliant Blue R-250.

Assay of enzyme activity and protein

Enzyme assays for the CDNB conjugation reactions were performed at 30 °C according to a published method [5,6]. Observed reaction velocities were corrected for spontaneous reaction rates when necessary. All initial velocities were determined in triplicate in buffers equilibrated at constant temperature. Catalytic-centre activities were calculated on the basis of one active site per subunit. Protein concentration was determined by the method of Bradford [26] using BSA (fraction V) as a standard.

Kinetic analysis

Steady-state kinetic measurements were performed at 30 °C in 0.1 M potassium phosphate buffer (pH 6.5). Initial velocities were determined in the presence of 2.5 mM GSH, and CDNB was used in the concentration range of 0.05–1.2 mM. Alternatively, CDNB was used at a fixed concentration (1 mM), and the GSH concentration was varied in the range of 0.4–10 mM. Solutions of GSH or analogues were freshly prepared each day and stored on ice under N_2.

Kinetic data were fitted to the equation, which is described by Lo Bello et al. [27], for the rapid equilibrium, random sequential Bi Bi model according to Scheme 1:

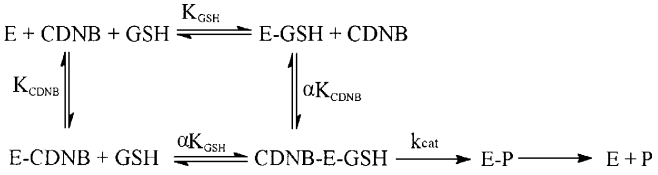

Scheme 1

where α is the coupling factor, K_{GSH} is the dissociation constant of GSH and K_{CDNB} is the dissociation constant for CDNB.

Inhibition experiments with methylglutathione were performed at ten substrate concentrations (50–500 μM GSH or CDNB) in the presence of fixed inhibitor concentrations ranging from 0.1–2 mM.

The apparent kinetic parameters k_{cat} and K_m were determined at a fixed GSH concentration with various CDNB concentrations, by fitting the collected steady-state data to the Michaelis–Menten equation by non-linear regression analysis using the GraFit (Erithacus Software, Ltd.) computer program.

Viscosity dependence of kinetic parameters

The effect of viscosity on kinetic parameters was assayed at 30 °C in 0.1 M potassium phosphate buffer (pH 6.5) containing variable glycerol concentrations. Viscosity values (η) at 30 °C were calculated as described by Wolf et al. [28].

Limited proteolysis of wild-type and mutant enzymes by trypsin

Limited proteolysis of wild-type GST and mutants $Ser^{11} \rightarrow Ala$, $His^{40} \rightarrow Ala$, $Lys^{41} \rightarrow Ala$, $Gln^{53} \rightarrow Ala$ and $Ser^{67} \rightarrow Ala$ by trypsin was performed at 25 °C, in 50 mM Tris/HCl buffer (pH 8.2) containing 10 mM $CaCl_2$. A suitable amount of enzyme was digested with 10% (w/w) trypsin. The rate of wild-type and mutant enzyme digestion was followed by periodically removing samples for assay of enzymic activity. Initial rates of inactivation were deduced from plots of log percentage of activity remaining versus time (min). Separation of the resulting peptides was achieved by HPLC analysis using a computerized Gilson gradient bioHPLC system and a gel-filtration column under denaturing conditions [Protein PAK 300SW; 300 mm × 7.8 mm (internal diam.); Waters, Milford, MA, U.S.A.]. The column was equilibrated with 100 mM potassium phosphate buffer (pH 6.5) containing 100 mM KCl and 8 M urea, and was calibrated using BSA, yeast alcohol dehydrogenase and horse heart cytochrome *c* as molecular mass markers. The digested enzymes were run isocratically at a flow rate of 0.03 ml/min. The effluents were monitored at 220 nm. Fractions of 0.5 ml were collected, and those with the desired peptide fragment were pooled, dialysed and subjected to manual amino acid sequencing as previously described [29].

Spectroscopic studies

Difference spectra of GSH bound to GST I were obtained with a PerkinElmer Lamda 16 double-beam double monochromator UV-visible spectrophotometer (PerkinElmer, Norwalk, CT, U.S.A.), equipped with a cuvette holder that was thermostated at 25 °C by a PTP-1 peltier temperature programmer (PerkinElmer). In a typical experiment 1 mM GSH (final concentration)

was added to GST I (approx. 10 μM active sites) in 1 ml of 0.1 M suitable buffer. The amount of thiolate formed at each pH was monitored using the peak-to-trough amplitude between 240 and 300 nm on the basis of a molar absorption coefficient at 240 nm of 5000 $M^{-1} \cdot cm^{-1}$ after subtraction of the spectral contributions of free enzyme and of free GSH, dissolved in BSA solution showing an A_{240} similar to that of the GST I sample. pK_a values were obtained as described in [6] by fitting the data to the following equation:

$$y = y_{lim}/(1 + 10^{pK_a - pH})$$

RESULTS

Protein expression and purification

Wild-type and mutants of GST I were expressed in high levels as soluble proteins in *E. coli*. The extra six histidine residues tagged on to the N-terminus of the recombinant enzyme enabled GST I to be rapidly purified by immobilized metal ion affinity chromatography. It was anticipated that some mutant enzymes would be devoid of GST activity or have reduced affinity for GSH, and hence be difficult to purify by affinity chromatography on an immobilized GSH affinity column. The wild-type and mutant enzymes were eluted from the column with 0.1 M imidazole, at pH 6.2. However, there were a few minor contaminating proteins, which were removed after re-chromatography of the eluted fractions. Kinetic comparison (results not shown) of the tagged and untagged enzyme showed that the extra six histidine residues on the N-terminus did not interfere with the activity and function of the enzyme.

Kinetic analysis of the GSH conjugation to CDNB with the wild-type enzyme

CDNB is generally considered to be the classical GST substrate, because most GST isoenzymes display high activity towards it. Although the kinetic mechanism of GSH conjugation to CDNB has been investigated for a number of GST isoenzymes [5–7], it is obvious that a steady-state kinetic characterization needs to be established prior to any other investigation concerning the catalytic mechanism of the θ class plant GST I.

When GSH was the variable substrate with several fixed concentrations of CDNB, a Lineweaver–Burk plot with intersecting lines was obtained (Figure 1A), and with CDNB as the variable substrate at fixed concentrations of GSH, an intersecting pattern was again obtained (Figure 1B). These data fitted well to either the simplest rapid equilibrium, random sequential Bi Bi equation or the mathematically equivalent steady-state ordered Bi Bi model. Product inhibition studies with methylglutathione allowed discrimination between the two possible mechanisms. Methylglutathione is a competitive inhibitor towards both GSH and CDNB. The re-plots of inhibition data are diagnostic for the rapid equilibrium model. The secondary plots of inhibition constants (K_i) versus GSH or CDNB derived from a set of reciprocal plots at different fixed concentrations of methylglutathione (0.1–2 mM) (with CDNB as the varied substrate and fixed GSH concentrations and vice versa) were linear over 15 substrate concentrations (50–500 μM for GSH and CDNB). Data from Figure 1 provide evidence of the convergence of the lines above the abscissa axis, showing a coupling factor $\alpha = 0.4 \pm 0.03$ with CDNB. This fractional number indicates the existence of intrasubunit structural communication between the GSH binding site (G-site) and the H-site, and that the affinity for GSH increases in the presence of CDNB by approx. 2.5-fold.

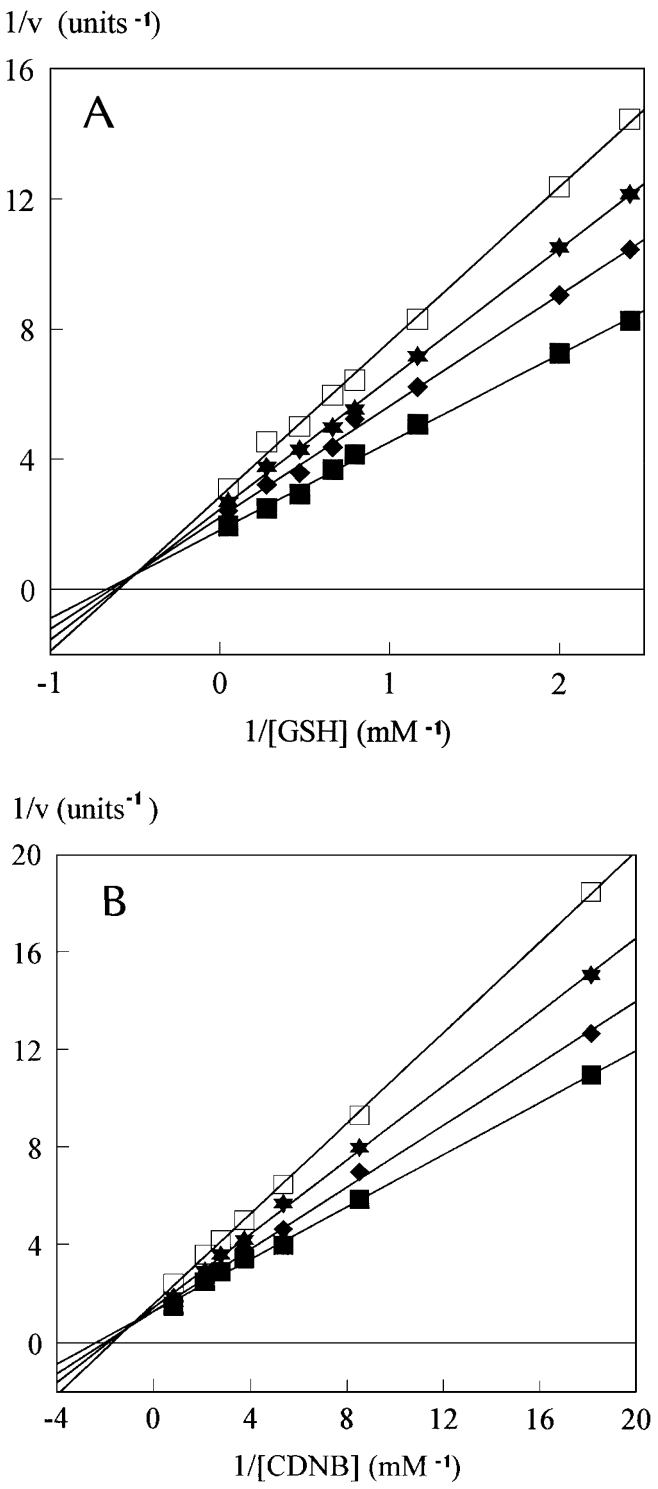

Figure 1 Initial velocity analysis of maize GST I at 30 °C in 0.1 M potassium phosphate buffer (pH 6.5)

(**A**) With GSH as the variable substrate for several fixed concentrations of CDNB: 0.165 mM (□); 0.33 mM (✱); 0.79 mM (◆); 1.15 mM (■). (**B**) With CDNB as the variable substrate for several fixed concentrations of GSH: 0.46 mM (□); 0.91 mM (✱); 2.19 mM (◆); 3.2 mM (■).

The dissociation constants of GSH and CDNB were determined as 1.6 mM and 2.2 mM respectively. Kinetic analysis of the Lys[41] → Ala mutant showed that the mutant follows the rapid equi-

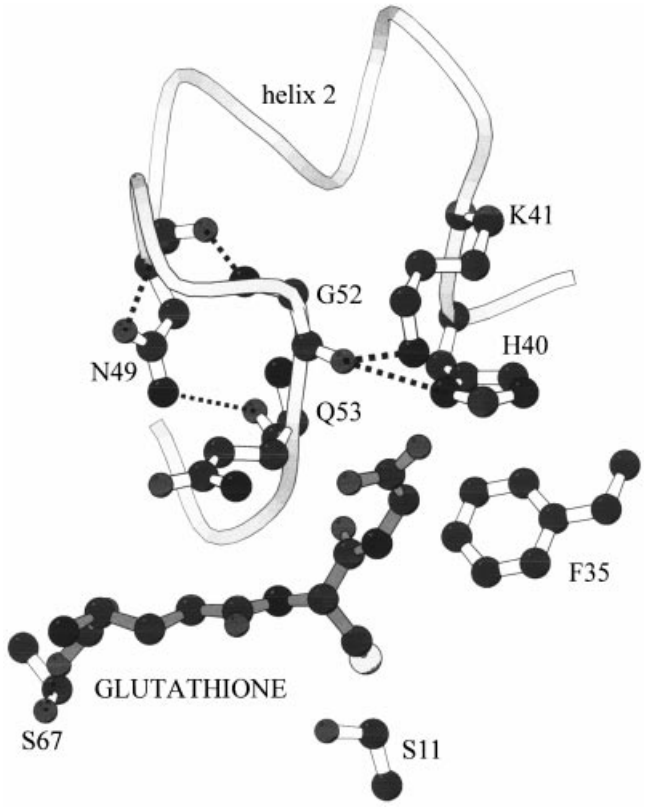

Figure 2 Diagram depicting mutated residues and other important nearby residues of maize GST I

Bound GSH is shown with dark-grey bonds to improve clarity. The Figure was made using Molscript [56].

librium model with a coupling factor of $\alpha = 0.7 \pm 0.05$, indicating that the structural communication has been altered in the mutated enzyme.

Addition of chloride ions (in the form of KCl) at concentrations up to 100 mM gave no significant inhibition of initial rates when GSH and CDNB were fixed at 5 mM and 1.5 mM respectively. The lack of inhibition by chloride ions indicates that little specificity exists for the leaving group from the electrophile. This is consistent with the broad specificity of GSTs, resulting in a variety of leaving groups [1]. Since methylglutathione gave a competitive pattern with respect to GSH and CDNB, it is likely that the product *S*-(2,4-dinitro-phenyl)glutathione leaves after chloride, if release is ordered or, alternatively, in random order.

Kinetic analysis of the effect of replacement of GSH binding residues on CDNB conjugation reactions

On the basis of the available X-ray crystal structure of GST I [11,13] five residues (Ser^{11}, His^{40}, Lys^{41}, Gln^{53} and Ser^{67}; Figure 2) from the GSH binding pocket were selected for assessment of their contribution to substrate binding and catalysis. These residues were individually mutated to alanine. The kinetic parameters k_{cat} and K_m determined by steady-state kinetic analysis are listed in Table 1. All the mutants showed increased K_m values for GSH, whereas the mutants $His^{40} \rightarrow Ala$, $Lys^{41} \rightarrow Ala$ and $Gln^{53} \rightarrow Ala$ showed differences in K_m values for

Table 1 Steady-state kinetic parameters and pK_a values for the thiol group of GSH of wild-type and mutants of maize GST I for the CDNB conjugation reaction at pH 6.5 and 30 °C

Enzyme	K_m^{GSH} (mM)	K_m^{CDNB} (mM)	k_3 (% compared with wild-type)	pK_a
Wild-type	1.1 ± 0.2	1.6 ± 0.1	100	6.2 ± 0.10
$Ser^{11} \rightarrow Ala$	4.6 ± 0.2	1.9 ± 0.1	1.3	7.7 ± 0.13
$His^{40} \rightarrow Ala$	6.1 ± 0.3	2.3 ± 0.1	21.8	6.8 ± 0.11
$Lys^{41} \rightarrow Ala$	5.6 ± 0.4	5.1 ± 0.3	16.4	6.9 ± 0.10
$Gln^{53} \rightarrow Ala$	3.9 ± 0.2	0.2 ± 0.04*	9.7	6.8 ± 0.13
$Ser^{67} \rightarrow Ala$	1.8 ± 0.1	1.4 ± 0.05	23.1	6.3 ± 0.11

* The mutant $Gln^{53} \rightarrow Ala$ does not strictly obey Michaelis–Menten kinetics for CDNB binding. Thus K_m^{CDNB} should be considered as an apparent value.

CDNB when compared with the wild-type enzyme. In particular, the mutant $Lys^{41} \rightarrow Ala$ showed an increase of approx. 3.2-fold in its K_m value for CDNB, whereas the mutant $Gln^{53} \rightarrow Ala$ exhibited an 8-fold decrease in K_m for CDNB.

The effects on k_{cat} caused by the mutations were more significant. Dramatic differences were observed for mutants $Ser^{11} \rightarrow Ala$ and $Gln^{53} \rightarrow Ala$, which showed 77- and 10-fold decreases in k_{cat} values respectively. The mutants $His^{40} \rightarrow Ala$, $Lys^{41} \rightarrow Ala$ and $Ser^{67} \rightarrow Ala$ showed moderate decreases in k_{cat} values of between 4.1- and 6.1-fold, compared with that of the wild-type enzyme.

pH dependence of spectroscopic parameters

Direct demonstration of the formation of GSH thiolate at the active site and its dependence on pH has been studied by difference spectroscopy. The difference spectrum of the binary complex GST I–GSH shows an absorption band centred at 240 nm that is diagnostic of a thiolate anion (Figure 3A). The pH dependence of this spectral perturbation at 240 nm identifies an apparent pK_a of 6.2 for the bound thiol ionization (Figure 3B). To check the influence of the GSH binding residue on GSH thiol ionization, difference spectroscopy experiments were performed for the mutants $Ser^{11} \rightarrow Ala$, $His^{40} \rightarrow Ala$, $Lys^{41} \rightarrow Ala$, $Gln^{53} \rightarrow Ala$ and $Ser^{67} \rightarrow Ala$, and the results are shown in Table 1. $Ser^{11} \rightarrow Ala$ exhibits a dramatic increase in pK_a value for the bound GSH, approx. 1.5 pH units higher than that found for the wild-type enzyme. The mutants $His^{40} \rightarrow Ala$, $Lys^{41} \rightarrow Ala$ and $Gln^{53} \rightarrow Ala$ also exhibit increased pK_a values, whereas the mutant $Ser^{67} \rightarrow Ala$ does not seem to significantly change the pK_a of bound GSH.

Rate-limiting step in the GST I-catalysed reaction

The effect of viscosity on the kinetic parameters was measured in order to analyse the rate-limiting step of the catalytic reaction. A decrease in k_{cat} by increasing the medium viscosity should indicate that the rate-limiting step of the reaction is related to the product release or to diffusion-controlled structural transitions of the protein [30]. A plot of the inverse relative rate constant k^{o}_{cat}/k_{cat} (k^{o}_{cat} is determined at viscosity η^{o}; where ^{o} indicates that the values were obtained in the absence of glycerol) versus the relative viscosity, η/η^{o}, should be linear, with a slope equal to unity when the product release is limited by a strictly diffusional barrier or a slope approaching zero if chemistry or another non-diffusional barrier is rate-limiting [31]. The inverse relative rate constant k^{o}_{cat}/k_{cat} for the enzyme-catalysed reaction shows linear dependence on the relative viscosity with a slope (1.1 ± 0.05) very

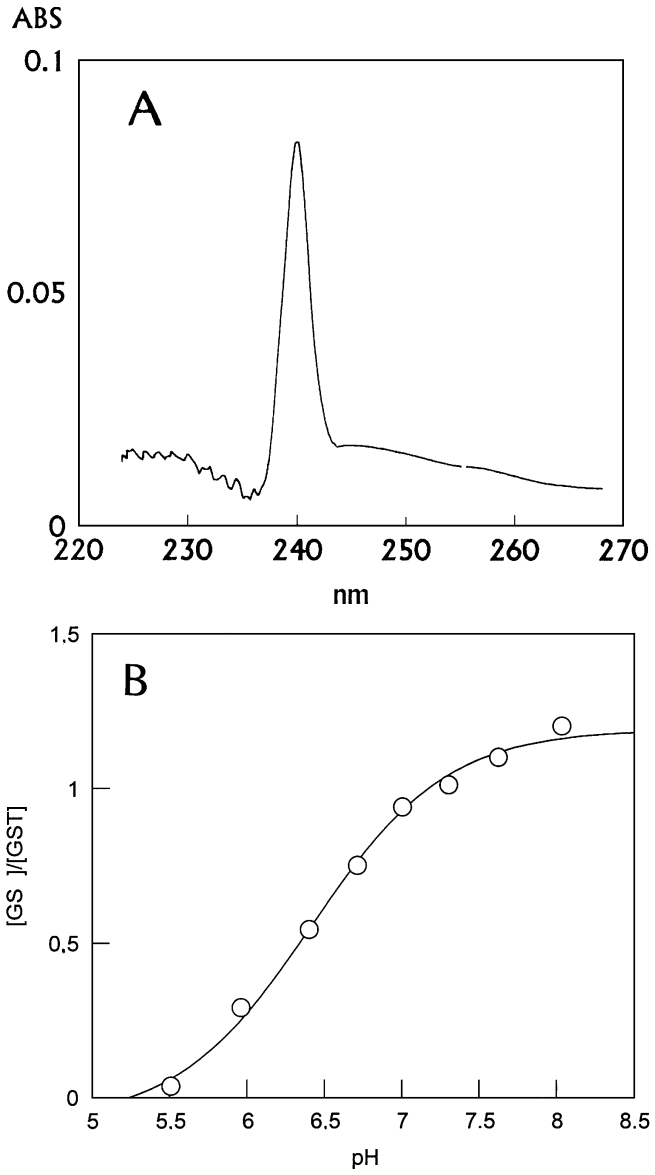

Figure 3 Spectroscopic evidence for the ionization of GSH in GST I

(**A**) Difference spectra of the wild-type GST I–GSH binary complex in 0.1 M potassium phosphate buffer (pH 7.3). (**B**) pH dependence of the thiolate anion of GSH (GS) in the GST I–GSH binary complex, obtained at different pH values. Each experimental point is the mean of three determinations.

close to unity, whereas the uncatalysed reaction is fully viscosity independent, as illustrated in Figure 4. In contrast the mutants $Ser^{11} \rightarrow Ala$, $His^{40} \rightarrow Ala$, $Lys^{41} \rightarrow Ala$ and $Gln^{53} \rightarrow Ala$ exhibited k_{cat} values with different degrees of viscosity dependence compared with the wild-type enzyme (Figure 4). The mutant $Ser^{67} \rightarrow Ala$ showed no appreciable difference compared with the wild-type enzyme. It is important to note that glycerol did not induce changes in the enzyme secondary structure as detected by far-UV difference spectroscopy (results not shown). Furthermore, glycerol did not have any non-specific inhibitory effect on catalysis.

The K_m for GSH is also affected by glycerol, whereas no change has been observed for K_m^{CDNB}. The effect of increased glycerol concentration on the K_m for GSH is diminished for the

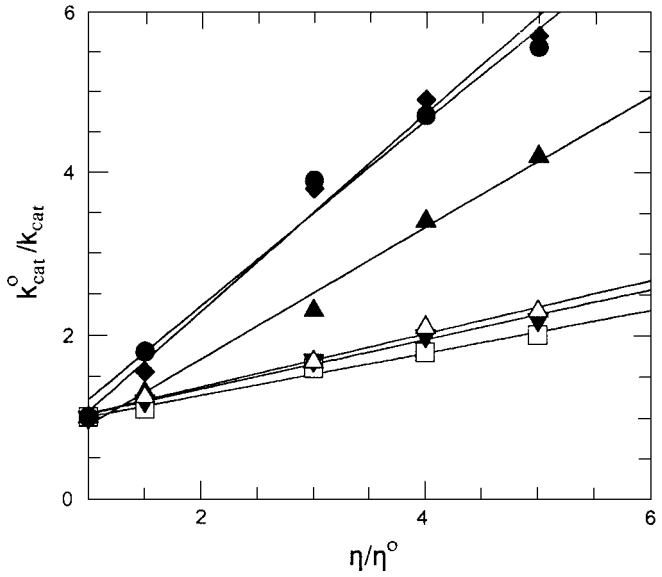

Figure 4 Effect of viscosity on kinetic parameters

Plot of the reciprocal of the relative catalytic-centre activity (k^0_{cat}/k_{cat}) as a function of relative viscosity (η/η^0) with glycerol as co-solvent for the wild-type enzyme (◆), and for the mutants $Ser^{11} \rightarrow Ala$ (▲), $His^{40} \rightarrow Ala$ (▼), $Lys^{41} \rightarrow Ala$ (□), $Gln^{53} \rightarrow Ala$ (Δ) and $Ser^{67} \rightarrow Ala$ (●). Experiments were performed in triplicate and the lines were calculated by least-squares regression analysis.

mutants $His^{40} \rightarrow Ala$, $Lys^{41} \rightarrow Ala$ and $Gln^{53} \rightarrow Ala$ compared with wild-type. In particular, the K_m for GSH of the wild-type enzyme was reduced 8.7-fold at 50% glycerol concentration, whereas in the mutants the same glycerol concentration led to decreases of approx. 3–4-fold.

Limited proteolysis of wild-type and mutant enzymes by trypsin

Limited trypsin proteolysis experiments under non-denaturing conditions of wild-type and $Ser^{11} \rightarrow Ala$, $His^{40} \rightarrow Ala$, $Lys^{41} \rightarrow Ala$, $Gln^{53} \rightarrow Ala$ and $Ser^{67} \rightarrow Ala$ mutant enzymes were performed in order to characterize the main peptide bond that is the target for trypsin. Analysis of protein digests on an HPLC column, in the presence of 8 M urea, gave two main peptide fragments. N-terminal sequence analysis gave the sequence Met-Ala-Pro for the larger fragment that eluted at 65 min (P1) and Ser-Pro-Glu for the smaller fragment that eluted at 67.5 min (P2). The N-terminal amino acid sequence of the P1 fragment corresponds to the amino acids of fragment 42–208, whereas the N-terminal amino acid sequence of the P2 fragment corresponds to the fragment 1–41. From these experiments it becomes clear that the main target of trypsin is the peptide bond between Lys^{41} and Ser^{42}. Lys^{44}, the structural equivalent of Lys^{41} in human GST P1-1, has also been confirmed as a sole point of attack by trypsin [32].

The rate of proteolytic cleavage was accompanied by a concomitant loss of enzyme activity of wild-type and mutant enzymes as shown in Table 2. Comparison of the rate of inactivation shows that the mutant $Lys^{41} \rightarrow Ala$ exhibits an approx. 25-fold lower proteolysis rate, compared with the wild-type enzyme, supporting the conclusion that the main target of trypsin is the peptide bond between Lys^{41} and Ser^{42}. $His^{40} \rightarrow Ala$ exhibits a proteolysis rate approx. 14-fold higher, whereas the mutant $Gln^{53} \rightarrow Ala$ shows a 15-fold lower proteolysis rate, compared with the wild-type enzyme. In contrast, the mutants

Table 2 Proteolytic susceptibility of wild-type and mutants of GST I

Enzyme inactivation rates were calculated in the linear part of the time course reaction.

Enzyme	$10^{-3} \times$ Inactivation rate (min^{-1})
Wild-type	12.4
$Ser^{11} \rightarrow Ala$	13.6
$His^{40} \rightarrow Ala$	165.6
$Lys^{41} \rightarrow Ala$	0.49
$Gln^{53} \rightarrow Ala$	0.81
$Ser^{67} \rightarrow Ala$	14.5

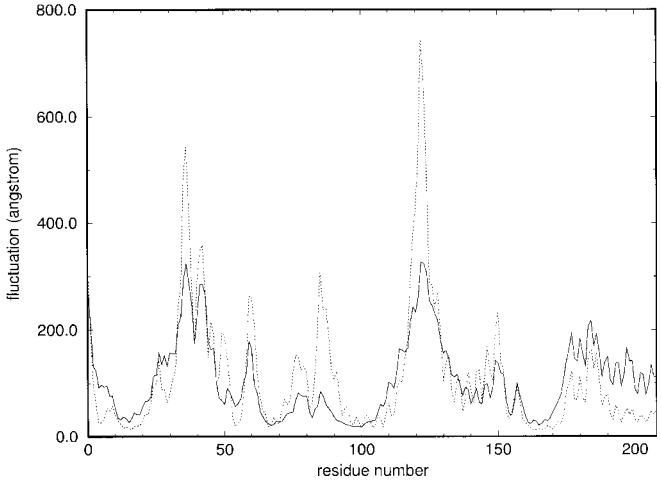

Figure 5 Fluctuation of C_α atoms produced by CONCOORD

Continuous line, GST I dimer; broken line, GST I monomer.

$Ser^{11} \rightarrow Ala$ and $Ser^{67} \rightarrow Ala$ showed no appreciable difference in the inactivation rate, compared with the wild-type enzyme.

Computer simulations

Computational analyses were then performed with the aim of better understanding the main structural fluctuations of the protein molecule.

The first step was to check if the flexibility present in α-helix 2 in simulations of the monomer structure [33,34] was still present in dimer simulations. Thus CONCOORD was applied both to monomer and dimer structures. The results showed that the high flexibility of α-helix 2 in the monomer structure was reduced for the dimer simulations of both human P1-1 (results not shown) and maize GST I structures (Figure 5). This indicates that the presence of one subunit restricts the dynamics of the other. Hence it is important to simulate the entire dimer.

The results obtained suggest that the short 3_{10}-helical segment of α-helix 2 (residues 35–46), which contains conserved residues from the G-site (e.g. His^{40} and Lys^{41}) and the H-site (Phe^{35}), and α-helix 3‴ (residues 118–122), which contains conserved residues from the H-site (e.g. Ile^{118}, Met^{121} and Leu^{122}), exhibit the highest degrees of structural mobility (Figure 5). These regions are among those showing highest mobility in the first eigenvector of the essential dynamics analysis, which represents the largest essential motion.

DISCUSSION

Steady-state kinetic analysis

Kinetic studies have been performed and presented in this report in order to characterize the structural and functional roles of GSH binding residues of maize GST I. Kinetic data reported in the present study suggest that the GST I-catalysed reaction between CDNB and GSH follows a rapid equilibrium, random sequential Bi Bi kinetic mechanism. The kinetic mechanism of the GST-catalysed conjugation reaction is quite complex and isoenzyme-dependent. For example, the π class GST follows a rapid equilibrium random Bi Bi kinetic mechanism [5,35], whereas a steady-state random Bi Bi kinetic mechanism was proposed for rat GSTs M1-1, M1-2 and A3-3 [36,37] and octopus hepatopancreatic GST [38]. In the case of θ class, for the rat GST T2-2 a hysteric reaction mechanism was suggested based on presteady-state and steady-state kinetics [39], whereas for the *Lucilia cuprina* enzyme, a steady-state random Bi Bi mechanism was proposed to explain the non-Michaelian substrate rate curves [6].

With CDNB an intrasubunit modulation of one substrate on the binding of the second one was observed with a coupling factor of $\alpha = 0.4$. This indicates the existence of intrasubunit structural communication between the G- and H-sites. Kinetic analysis of the $Lys^{41} \rightarrow Ala$ mutant shows a coupling factor of $\alpha = 0.7$, indicating that the structural communication has been reduced after mutation. One hypothesis to explain this kinetic difference observed between wild-type and mutant $Lys^{41} \rightarrow Ala$ is the following. Crystallographic studies [11,12] have shown that binding of GSH to GST I leads to conformational changes in the 3_{10}-helical segment of residues 35–45, that allows Lys^{41} to adopt its correct conformation for direct interaction with the glycine carboxylate of GSH. These conformational changes are presumably transmitted to Phe^{35} (Figure 2), which is located in the same flexible segment and directly contributes to the H-site, thereby enabling it to adopt its correct conformation for productive binding of the electrophile substrate. Mutation of Lys^{41} to alanine removes all possible interactions of residue 41 with GSH and may restrict or inhibit the conformational changes of the helical segment that modulate Phe^{35} conformation.

Substitution of the chlorine by the more electronegative fluorine in the CDNB molecule increases the second-order rate constant of the uncatalysed reaction with GSH by approx. 50-fold, suggesting that σ-complex formation is rate limiting [30,40]. If decomposition of the σ-complex to product is rate-limiting then the opposite effect is expected because of the stronger C–F bond [40]. Our kinetic data suggest that maize GST I is insensitive to the nature of the leaving group ($k_{cat}^{FDNB}/k_{cat}^{CDNB} = 1.2$; where FDNB corresponds to 1-fluoro-2,4-dinitrobenzene), indicating that a non-chemical step may be rate limiting in the enzymic reaction. In the catalytic reaction the value of k_{cat}/K_m ($10^5\ s^{-1} \cdot M^{-1}$) is well below the value beyond which substrate binding is considered to be rate limiting ($10^9\ s^{-1} \cdot M^{-1}$). The low pK_a value of the bound thiolate anion ($pK_a = 6.2$, see below) rules out the ionization of the thiol group of GSH as a rate-limiting process. The dependence of k_{cat} on the medium viscosity indicates that the catalytic-centre activity of GST I is limited by the rate of product release. A plot of the inverse relative rate constant versus the relative viscosity (Figure 4) gave a straight line with a slope close to unity, indicating that release of product is limited by a strictly diffusional barrier [30,31]. The possibility that glycerol modifies the structure of the enzyme may be ruled out as it is not supported by far-UV difference spectra, which in the presence or absence of glycerol, are indistinguishable. Diffusion controlled phenomena of the protein have already

been reported to modulate the catalysis of other GST isoenzymes: a conformational change in the case of the ternary complex of human P1-1 [5], and product release for rat GST M1-1 [30], *L. cuprina* GST [6], rat GST T2-2 [39] and α class GSTs [41].

Computer simulations

Dynamic simulations performed in the present study have shown that the short 3_{10}-helical segment of α-helix 2 undergoes large conformational changes, which seem to be related to the modulation of the affinity of the G-site for GSH (via interaction of His^{40} and Lys^{41} with GSH), and the affinity of the H-site for the electrophile substrate (via interaction with Phe^{35}). The other segment of protein with high mobility is the α-helix 3‴, containing conserved key residues of the hydrophobic binding site (Phe^{114}, Ile^{118}, Met^{121} and Leu^{122}), which may also influence binding of the electrophile substrate. The flexibility of this part of the H-site may be modulated by Gly^{123} and/or Gly^{124}. Gly^{123} is conserved among all plant θ class GSTs, but is absent in the other classes of GST. This part of the molecule exhibits the more dramatic differences when compared with the dynamics of human GST P1-1 [33,34]. This may be due to the absence of these glycine residues from the human enzyme and may be related to the wide substrate specificity of the plant enzyme, and to its preference for large hydrophobic substrates.

Effects of point mutations on GSH thiol ionization

The crucial property of GSTs is their ability to lower the pK_a of the thiol group of the bound GSH. Published work shows that the pK_a of GSH in the active site ranges from 6.0 to 6.5 [6,40–44]. The lowering of this pK_a value is accomplished by Tyr^6 in rat GST [40], Tyr^7 in human GST P1-1 [43], Tyr^8 in human GST A1-1 [44] and Ser^9 in the θ class GST from *L. cuprina* [6]. The corresponding residue in GST I is Ser^{11}. Direct evidence for the contribution of Ser^{11} to the forced deprotonation and stabilization of bound GSH comes from the UV difference spectroscopic studies. The ionization of free GSH in the reaction with CDNB exhibits a pK_a of 8.7 [44]. The native enzyme gives a pK_a for the bound GSH of 6.2, whereas the mutant $Ser^{11} \rightarrow Ala$ gives an apparent pK_a of 7.7 and exhibits a catalytic efficiency of 1.3 % compared with that of the wild-type enzyme for the CDNB reaction. The catalytic role of the hydroxy group of Ser^{11} may be the donation of a hydrogen bond to the negatively charged thiolate anion of bound GSH, enhancing its nucleophilicity and stability in accordance with the role of Ser^9 in the *L. cuprina* enzyme [6].

The amino acid residues His^{40}, Lys^{41} and Gln^{53} also seem to contribute to GSH ionization (Table 1). There are two possibilities concerning the contribution of these residues to thiol ionization. These residues, in particular the positively charged residues His^{40} and Lys^{41}, may directly contribute to the electrostatic field of the active site. The GSH is immersed in an electrostatically positive region in GST I, due to three positively charged residues (His^{40}, Lys^{41} and Arg^{68}) and the partial positive charge associated with the N-terminus of α-helix 1. This positive electrostatic field in the G-site is characteristic of all GSTs and has been suggested, based on theoretical computational studies [45], to contribute to thiol ionization. The other possibility, which may be more relevant to the uncharged Gln^{53}, arises from the perturbations in the enzyme structure induced by the mutations (e.g. the structure of α-helix 2, see below), which may indirectly influence the electrostatic field of the active site.

The involvement of positively charged residues in the regulation of the electrostatic field has also been observed in other GSTs. For example, residues His^{107}, Arg^{107} and Arg^{15} from human GST 1a-1a [46], human GST M2 [47] and human GST A1-1 [48] respectively, have been shown to contribute to active-site ionization.

Effects of point mutations on k_{cat} and K_m

The dramatic reduction in k_{cat}, caused by the mutations, may be due to their contributions to product release (the rate-limiting step), as shown in Figure 4. The intermediate values of the slopes ($0 < \text{slope} < 1$) observed in the mutants $Ser^{11} \rightarrow Ala$, $His^{40} \rightarrow Ala$, $Lys^{41} \rightarrow Ala$ and $Gln^{53} \rightarrow Ala$ indicate that the rate-limiting step in the mutants is not strictly dependent on a diffusional barrier, and other viscosity-dependent motions or conformational changes of the mutated proteins contribute to the rate-limiting step of the catalytic reaction [30]. Probably, the structural integrity or flexibility of functionally important regions of the mutated enzymes has been altered. One region of probable importance is the 3_{10}-helical segment of α-helix 2.

Several pieces of evidence indicate that the 3_{10}-helical segment of α-helix 2 is a flexible region in maize GST I: it has the highest crystallographic temperature factors of the structure [11]; it undergoes the largest C_α fluctuations as observed by molecular dynamic simulations analysis (Figure 5); it offers the sole point of attack (Lys^{41}) for the proteolytic cleavage by trypsin; and point mutations in the α-helix 2 region (e.g. $His^{40} \rightarrow Ala$ and $Gln^{53} \rightarrow Ala$) dramatically change the rate of proteolysis (by approx. 208-fold). A correlation between sites of limited proteolysis and sites of high segmental mobility has been suggested by numerous experimental studies in globular proteins [49,50]. It has been observed that limited proteolysis under non-denaturing conditions occurs at flexible loops. The increase in the rate of proteolysis induced by the mutation $His^{40} \rightarrow Ala$ and the decrease in the rate of proteolysis induced by the mutation $Gln^{53} \rightarrow Ala$ may therefore be explained by supposing that the 3_{10}-helical segment becomes more flexible and probably more exposed to the solvent in the former mutant, whereas its flexibility is restricted in the latter. The high flexibility of α-helix 2 and its involvement in the catalytic mechanism of human GST P1-1 has also been reported [51].

Other possible factors that may contribute to the reduction of k_{cat} in the mutated enzymes are a shift in the pK_a of the -SH group, and the involvement of the mutated amino acids in the correct orientation of the GSH thiol group at the active site. These factors may be most relevant in the case of the $Ser^{11} \rightarrow Ala$ mutant, where the dramatic reduction in k_{cat} observed after mutation cannot be correlated to the flexibility of the 3_{10}-helical segment. Recently, Tyr^9 and Ser^{11}, the structurally equivalent residues of maize GST I Ser^{11}, in rat GSTA1-1 [52] and rat GST T2-2 [53] respectively, have been reported to play important roles in efficient product release and in controlling the C-terminal dynamics. Presumably the same role may be attributed to Ser^{11} in maize GST I.

The K_m for GSH of the wild-type enzyme is reduced by 8.7-fold at 50 % glycerol concentration, whereas the mutants $His^{40} \rightarrow Ala$, $Lys^{41} \rightarrow Ala$ and $Gln^{53} \rightarrow Ala$ exhibit decreases in K_m for GSH of approx. 3–4-fold, at the same glycerol concentration. One possible explanation is based on the diffusion-controlled motions of the 3_{10}-helical segment of α-helix 2. The presence of viscosigen may increase the rigidity of the helical segment leading to a 'freezing' of the highly mobile GSH molecule in its more productive conformation. This is not feasible to the same extent in the cases of the $His^{40} \rightarrow Ala$, $Lys^{41} \rightarrow Ala$ and $Gln^{53} \rightarrow Ala$ mutants because of the detrimental effects of the mutations on the structural integrity or flexibility of the 3_{10}-helical segment.

The contribution of His^{40}, Lys^{41} and Gln^{53} to K_m values for the electrophile substrate may be relevant to the indirect effect of these residues on the H-site architecture. The perturbation of the structure/flexibility of the 3_{10}-helical segment, as it has been already discussed, may affect the conformation of the key residue Phe^{35}, which is part of this helical segment, and contributes part of the H-site (the mutant $Phe^{35} \rightarrow Leu$ showed an increase of approx. 20-fold in its K_m value for CDNB; N. E. Labrou and Y. D. Clonis, unpublished work). In addition, His^{40} is involved in a direct amino-aromatic interaction with Phe^{35} (Figure 2). The close proximity of an aromatic side chain to a charged histidine ring has been found to have certain structural and mechanistic implications, such as the increase of approx. 4 kJ/mol stabilizing energy and the elevation of the pK_a value of the histidine residue [54,55]. This probably accounts for the reduced thermal stability of the $His^{40} \rightarrow Ala$ mutant, compared with the wild-type enzyme (results not shown). The mechanistic implication is that the raised pK_a of histidine stabilizes its side-chain protonated form, which allows its side chain to interact more strongly with GSH carboxylate, contributing to the correct orientation of the substrate.

In conclusion, in the present study we have addressed questions regarding the functional and structural roles of GSH binding residues of GST I, by site-directed mutagenesis and dynamic studies. The results of the present work have practical significance, since they will form the basis for the rational design of new engineered GST I with altered substrate specificity and enhanced activity towards electrophile herbicides.

This work was supported by the Hellenic General Secretariat for Research and Technology (programme PENED-99, grant number 99ED70). We thank Dr D. Rigden for critical review of the manuscript before its submission.

REFERENCES

1 Edwards, R., Dixon, D. P. and Walbot, V. (2000) Plant glutathione S-transferases: enzymes with multiple functions in sickness and in health. Trends Plant Sci. **5**, 193–198

2 Armstrong, R. N. (1998) Mechanistic imperatives for the evolution of glutathione transferases. Curr. Opin. Chem. Biol. **2**, 618–623

3 Armstrong, R. N. (1997) Structure, catalytic mechanism, and evolution of the glutathione transferases. Chem. Res. Toxicol. **10**, 2–18

4 Lu, Y.-P., Li, Z.-S. and Rea, P. A. (1997) *AtMRP1* gene of Arabidopsis encodes a glutathione S-conjugate pump: isolation and functional definition of a plant ATP-binding cassette transporter gene. Proc. Natl. Acad. Sci. U.S.A. **94**, 8243–8248

5 Caccuri, A., Ascenzi, P., Antonini, G., Parker, M., Oakley, A., Chiessi, E., Nuccetelli, M., Battistoni, A., Bellizia, A. and Ricci, G. (1996) Structural flexibility modulates the activity of human glutathione transferase P1-1. Influence of a poor co-substrate on dynamics and kinetics of human glutathione transferase. J. Biol. Chem. **271**, 16193–16198

6 Caccuri, A., Antonini, G., Nicotra, M., Battistoni, A., Lo Bello, M., Board, P., Parker, M. and Ricci, G. (1997) Catalytic mechanism and role of hydroxyl residues in the active site of theta class glutathione S-transferases. Investigation of Ser-9 and Tyr-113 in a glutathione S-transferase from the Australian sheep blowfly, *Lucilia cuprina*. J. Biol. Chem. **274**, 29681–29686

7 Caccuri, A. M., Lo Bello, M., Nuccetelli, M., Nicotra, M., Rossi, P., Antonini, G., Federici, G. and Ricci, G. (1998) Proton release upon glutathione binding to glutathione transferase P1-1: kinetic analysis of a multistep glutathione binding process. Biochemistry **37**, 3028–3034

8 Roxas, V. P., Smith, Jr R. K., Allen, E. R. and Allen, R. D. (1997) Overexpression of glutathione S-transferase/glutathione peroxidase enhances the growth of transgenic tobacco seedlings during stress. Nat. Biotechnol. **10**, 988–991

9 Sommer, A. and Boger, P. (1999) Characterization of recombinant corn glutathione S-transferase isoforms I, II, III and IV. Pestic. Biochem. Physiol. **63**, 127–138

10 Reinemer, P., Prade, L., Hof, P., Neuefeind, T., Huber, R., Zettl, R., Palme, K., Schell, J., Koelln, I., Bartunik, H. and Beiseler, B. (1996) Three-dimensional structure of glutathione S-transferase from *Arabidopsis thaliana* at 2.2 Å resolution: structural characterization of herbicide-conjugating plant glutathione S-transferases and a novel active site architecture. J. Mol. Biol. **255**, 289–309

11 Neuefeind, T., Huber, R., Dasenbrock, H., Prade, L. and Bieseler, B. (1997) Crystal structure of herbicide-detoxifying maize glutathione S-transferase-I in complex with lactoylglutathione: evidence for an induced-fit mechanism. J. Mol. Biol. **274**, 446–453

12 Neuefeind, T., Huber, R., Reinemer, P., Knablein, J., Prade, L., Mann, K. and Bieseler, B. (1997) Cloning, sequencing, crystallization and X-ray structure of glutathione S-transferase-III from *Zea mays* var. mutin: a leading enzyme in detoxification of maize herbicides. J. Mol. Biol. **274**, 577–587

13 Prade, L., Huber, R. and Bieseler, B. (1998) Structures of herbicides in complex with their detoxifying enzyme glutathione S-transferase – explanations for the selectivity of the enzyme in plants. Structure (London) **6**, 1445–1452

14 Pemble, S. E. and Taylor, J. B. (1992) An evolutionary perspective on glutathione transferases inferred from class-Theta glutathione transferase cDNA sequences. Biochem. J. **287**, 957–963

15 Widersten, M., Kolm, R. H., Bjornestedt, R. and Mannervik, B. (1992) Contribution of five amino acid residues in the glutathione-binding site to the function of human glutathione transferase P1-1. Biochem. J. **285**, 377–381

16 Grove, G., Zarlengo, R. P., Timmerman, K. P., Tam, M. F. and Tu, C.-P. D. (1988) Characterization and heterospecific expression of cDNA clones of genes in the maize GSH S-transferase multigene family. Nucleic Acids Res. **16**, 425–438

17 Deng, W. P. and Nickoloff, J. A. (1992) Site-directed mutagenesis of virtually any plasmid by eliminating a unique site. Anal. Biochem. **200**, 81–90

18 Labrou, N. E., Rigden, D. J. and Clonis, Y. D. (2000) Characterization of the NAD^+ binding site of *Candida boidinii* formate dehydrogenase by affinity labelling and site-directed mutagenesis. Eur. J. Biochem. **267**, 6657–6664

19 Labrou, N. E. and Rigden, D. J. (2001) Active-site characterization of *Candida boidinii* formate dehydrogenase. Biochem. J. **354**, 455–463

20 de Groot, B. L., van Aalten, D. M. F., Scheek, R. M., Amadei, A., Vriend, G. and Berendsen, H. J. C. (1997) Prediction of protein conformational freedom from distance constraints. Proteins **29**, 240–251

21 de Groot, B. L., Vriend, G. and Berendsen, H. J. C. (1999) Conformational changes in the chaperonin GroEL: new insights into the allosteric mechanism. J. Mol. Biol. **286**, 1241–1249

22 Reinemer, P., Dirr, H. W., Ladenstein, R., Huber, R. and Lo Bello, M. (1992) Three-dimensional structure of class pi glutathione S-transferase from human placenta in complex with S-hexylglutathione at 2.8 Å resolution. J. Mol. Biol. **227**, 214–226

23 Amadei, A., Linssen, A. B. M. and Berendsen, H. J. C. (1993) Essential dynamics of proteins. Proteins **17**, 412–425

24 Ichiye, T. and Karplus, M. (1991) Collective motions in proteins: a covariance analysis of atomic fluctuations in molecular dynamics and normal mode simulations. Proteins **11**, 205–217

25 Laemmli, U. K. (1970) Cleavage of structural proteins during the assembly of the head of bacteriophage T4. Nature (London) **227**, 680–685

26 Bradford, M. A. (1976) A rapid and sensitive method for the quantitation of microgram quantities of protein utilizing the principle of protein-dye binding. Anal. Biochem. **72**, 248–254

27 Lo Bello, M., Oakley, A., Battistoni, A., Mazzetti, A., Nuccetelli, M., Mazzarese, G., RossJohn, J., Parker, M. and Ricci, G. (1997) Multifunctional role of Tyr 108 in the catalytic mechanism of human glutathione transferase P1-1. Crystallographic and kinetic studies on the Y108F mutant enzyme. Biochemistry **36**, 6207–6217

28 Wolf, A. V., Brown, M. G. and Prentiss, P. G. (1985) in Handbook of Chemistry and Physics (Weast, R. C., Astle, M. J. and Beyer, W. H., eds.), pp. D-219–D-269, CRC Press, Inc., Boca Raton, FL

29 Yarwood, A. (1989) Manual methods of protein sequencing. In Protein Sequencing: A Practical Approach (Findlay, J. B. C. and Geisow, M. J., eds.), pp. 119–145, Oxford University Press, Oxford

30 Johnson, W. W., Liu, S., Ji, X., Gilliland, G. L. and Armstrong, R. N. (1993) Tyrosine 115 participates both in chemical and physical steps of the catalytic mechanism of a glutathione S-transferase. J. Biol. Chem. **268**, 11500–11511

31 Sampson, N. S. and Knowles, J. R. (1992) Segmental motion in catalysis: investigation of a hydrogen bond critical for loop closure in the reaction of triosephosphate isomerase. Biochemistry **31**, 8488–8494

32 Lo Bello, M., Battistoni, A., Mazzetti, A., Board, P. G., Muramatsu, M., Federici, G. and Ricci, G. (1995) Site-directed mutagenesis of human glutathione transferase P1-1. Spectral, kinetic, and structural properties of Cys-47 and Lys-54 mutants. J. Biol. Chem. **270**, 1249–1253

33 Stella, L., Nicotra, M., Ricci, G., Nicola, R. and Di Iorio, E. E. (1999) Molecular dynamics simulations of human glutathione transferase P1-1: analysis of the induced-fit mechanism by GSH binding. Proteins, **37**, 1–9

34 Stella, L., Di Iorio, E. E., Nicotra, M. and Ricci, G. (1999) Molecular dynamics simulations of human glutathione transferase P1-1: conformational fluctuations of the apo-structure. Proteins **37**, 10–19

35 Phillips, M. F. and Mantle, T. J. (1991) The initial-rate kinetics of mouse glutathione *S*-transferase YfYf. Evidence for an allosteric site for ethacrynic acid. Biochem. J. **275**, 703–709

36 Ivanetich, K. M., Goold, R. D. and Sikakana, C. N. T. (1990) Explanation of the non-hyperbolic kinetics of the glutathione S-transferases by the simplest steady-state random sequential Bi Bi mechanism. Biochem. Pharmacol. **39**, 1999–2004
37 Jakobson, I., Warholm, M. and Mannervik, B. (1979) The binding of substrates and a product of the enzymatic reaction to glutathione S-transferase A. J. Biol. Chem. **254**, 7085–7089
38 Tang, S.-S. and Chang, G.-G. (1975) Steady-state kinetics and chemical mechanism of octopus hepatopancreatic glutathione transferase. Biochem. J. **309**, 347–353
39 Jemth, P. and Mannervik, B. (1999) Fast product formation and slow product release are important features in a hysteric reaction mechanism of glutathione transferase T2-2. Biochemistry **38**, 9982–9991
40 Liu, S., Zhang, P., Ji, X., Johnson, W. W., Gilliland, G. L. and Armstrong, R. N. (1992) Contribution of tyrosine 6 to the catalytic mechanism of isoenzyme 3-3 of glutathione S-transferase. J. Biol. Chem. **267**, 4296–4299
41 Allardyce, C. S., McDonagh, P. D., Lian, L.-Y., Wolf, C. R. and Roberts, G. C. K. (1999) The role of tyrosine-9 and the C-terminal helix in the catalytic mechanism of Alpha-class glutathione S-transferases. Biochem. J. **343**, 525–531
42 Chem, W. J., Graminski, G. F. and Armstrong, R. (1988) Dissection of the catalytic mechanism of isozyme 4-4 of glutathione S-transferase with alternative substrates. Biochemistry **27**, 647–654
43 Kong, K.-H., Takasu, K., Inoue, H. and Takahashi, K. (1992) Tyrosine-7 in human class Pi glutathione S-transferase is important for lowering the pKa of the thiol group of glutathione in the enzyme-glutathione complex. Biochem. Biophys. Res. Commun. **184**, 194–197
44 Stenberg, G., Board, P. G. and Mannervik, B. (1991) Mutation of an evolutionarily conserved tyrosine residue in the active site of a human class Alpha glutathione transferase. FEBS Lett. **293**, 153–155
45 Karshikoff, A., Reinemer, P., Huber, R. and Ladenstein, R. (1993) Electrostatic evidence for the activation of the glutathione thiol by Tyr7 in pi-class glutathione transferases. Eur. J. Biochem. **215**, 663–670
46 Patskovsky, Y. V., Patskovska, L. N. and Listowsky, I. (1999) Functions of His107 in the catalytic mechanism of human glutathione S-transferase hGSTM1a-1a. Biochemistry **38**, 1193–1202
47 Patskovsky, Y. V., Patskovska, L. N. and Listowsky, I. (2000) The enhanced affinity for thiolate anion and activation of enzyme-bound glutathione is governed by an arginine residue of human Mu class glutathione S-transferases. J. Biol. Chem. **275**, 3296–3304
48 Björnestedt, R., Stenberg, G., Widersten, M., Board, P., Sinning, I., Jones, T. A. and Mannervik, B. (1995) Functional significance of arginine 15 in the active site of human class alpha glutathione transferase A1-1. J. Mol. Biol. **247**, 765–773
49 Fontana, A., Polverino de Laureto, P. and De Filippis, V. (1993) Molecular aspects of proteolysis of globular proteins. In Protein Stability and Stabilization (van den Tweel, W., Harder, A. and Buitelear, M., eds.), pp. 101–110, Elsevier Science Publishers, Amsterdam
50 Fontana, A., Zambonin, M., Polverino de Laureto, P., De Filippis, V., Clemanti, A. and Scaramella, E. (1997) Probing the conformational state of apomyoglobin by limited proteolysis. J. Mol. Biol. **266**, 223–230
51 Ricci, G., Caccuri, A. M., Lo Bello, M., Rosato, N., Mei, G., Nicotra, M., Chiessi, E., Mazzetti, A. P. and Federici, G. (1996) Structural flexibility modulates the activity of human glutathione transferase P1-1. Role of helix 2 flexibility in the catalytic mechanism. J. Biol. Chem. **271**, 16187–16192
52 Nieslanik, B. S. and Atkins, W. M. (2000) The catalytic Tyr-9 of glutathione S-transferase A1-1 controls the dynamics of the C terminus. J. Biol. Chem. **275**, 17447–17451
53 Jemth, P. and Mannervik, B. (2000) Active site serine promotes stabilization of the reactive glutathione thiolate in rat glutathione transferase T2-2. J. Biol. Chem. **275**, 8618–8624
54 Loewenthal, R., Sancho, J. and Fersht, A. R. (1992) Histidine-aromatic interactions in barnase. Elevation of histidine pKa and contribution to protein stability. J. Mol. Biol. **224**, 759–770
55 Shoemaker, K. R., Fairman, R., Schultz, D. A., Robertson, A. D., York, E. J., Stewart, J. M. and Baldwin, R. L. (1990) Side-chain interactions in the C-peptide helix: Phe8 ... $His^{+}12$. Biopolymers **29**, 1–11
56 Kraulis, P. J. (1991) MOLSCRIPT: a program to produce both detailed and schematic plots of protein structures. J. Appl. Crystallogr. **24**, 946–950

Received 17 January 2001/23 March 2001; accepted 18 April 2001